Pergamon

Int. J. Heat Mass Transfer. Vol. 41, No. 1, pp. 73–80, 1998

Printed in Great Britain
0017–9310/98 $19.00+0.00

PII: S0017–9310(97)00104–X

Critical working frequency of reciprocating heat-transfer devices in axially reciprocating mechanisms

JIAN LING, YIDING CAO† and QIAN WANG

Department of Mechanical Engineering, Florida International University, Miami, FL 33199, U.S.A.

(*Received* 11 *June* 1996 *and in final form* 28 *March* 1997)

Abstract—The reciprocating heat-transfer device or reciprocating heat pipe has a high effective thermal conductance, and applications can be found in various reciprocating mechanisms, including offset cam mechanisms, Scotch yoke mechanisms, and piston assemblies of internal combustion engines. The liquid return mechanism presents the most important operating limitation for this type of heat-transfer device. In this paper, the potential applications of the reciprocating heat-transfer device to various reciprocating mechanisms are described. Theoretical analyses are performed for the critical working frequency of the device in connection with the reciprocating mechanisms. An analytical solution and semi-empirical correlation, with and without taking into account the flow resistance, are obtained. Extensive experiments for the critical working frequency are then undertaken on an engine tester. Comparison of the analytical and experimental results indicates that the analytical solutions and semi-empirical correlation provide an accurate prediction for the working limits of reciprocating heat-transfer devices. © 1997 Elsevier Science Ltd.

INTRODUCTION

The reciprocating heat pipe and its application in piston engines was first proposed by Cao and Wang [1] and Wang *et al.* [2]. Similar to conventional heat pipes [3–6], the reciprocating heat pipe is a liquid/vapor two-phase heat transfer device that has an evaporator at the heat input section and a condenser at the cooling section. The major difference between the conventional heat pipe and the reciprocating heat pipe is the liquid return mechanism from the condenser section to the evaporator section. The liquid condensate is returned from the condenser section to the evaporator section through the capillary force for wicked heat pipes, gravity for thermosyphons, and centrifugal force for rotating heat pipes. In wickless reciprocating heat pipes, however, the liquid return is achieved through the shaking-up of inertia force due to the axially reciprocating motion of the heat pipe. Extensive study has been made to understand the working mechanism of the heat pipe [2, 7, 8]. Investigations for the afore-mentioned heat pipe were conducted for a slider–crank mechanism of an internal combustion engine. However, the reciprocating heat pipe also has potential applications in many other reciprocating mechanisms, such as the cam-follower mechanism, offset slider–crank mechanism, harmonic motion mechanism, and Scotch yoke mechanism. Figure 1 schematically illustrates some potential applications of the reciprocating heat-transfer devices in various mechanisms. The locations where the heat transfer device could be installed are also indicated in the figure. Like many conventional heat pipes, the reciprocating heat pipe is subjected to certain working limitations. The most important working limitation for the current heat transfer device is the minimum reciprocating frequency of the reciprocating mechanisms, below which the liquid condensate cannot return from the condenser section to the evaporator

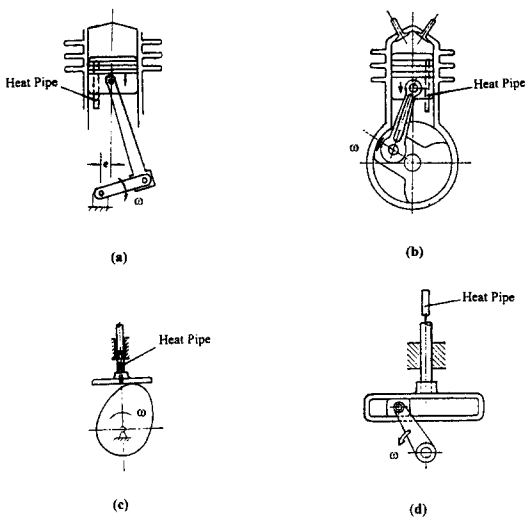

Fig. 1. Application background of reciprocating heat pipes: (a) engine with offset slider–crank mechanism; (b) engine with on-center slider–crank mechanism; (c) cam-follower mechanism; (d) scotch yoke mechanism.

† Author to whom correspondence should be addressed.

NOMENCLATURE

a	acceleration [m s^{-2}]
A_{hp}	cross-sectional area of heat pipe [m^2]
$A_{p,v}$	frontal area of liquid particle [m^2]
$A_{p,s}$	lateral area of heat pipe [m^2]
A_s	lateral area of liquid volume in heat pipe [m^2]
d	inner diameter of heat pipe [m]
D_h	hydraulic diameter [m]
e	offset of slider-crank mechanism [m]
F_R	mean resistant force acted on liquid particle in the time travel $t-t_0$ [N]
F_f	frictional force acted on liquid particle [N]
F_v	vapor drag force [N]
f_{min}	critical working frequency of heat pipe [Hz]
g	acceleration of gravity [m s^{-2}]
h	absolute displacement traveled by the liquid particle when the flow resistance is neglected [m]
h_0	absolute displacement traveled by the liquid particle from the separation point to the top end of the evaporator section [m]
h'	absolute displacement traveled by the liquid particle when the flow resistance is not neglected [m]
h_{fg}	latent heat of vaporization [J kg^{-1}]
k	location coefficient
l	length of piston connecting rod [m]
L	total length of heat pipe [m]
L_e	length of evaporator section [m]
L_l	height of liquid charge in heat pipe [m]
m_p	mass of liquid particle [kg]
m_l	mass of liquid in heat pipe [kg]
Pr	Prandtl number of saturated liquid
Q	heat input at evaporator section [W]
r	engine crank radius [m]
ratio	ratio of liquid volume to heat pipe volume
x_h	the upper dead end of heat pipe [m]
t	time [s]
u_m	mean velocity of liquid particle [m s^{-1}]
$u_{v,m}$	mean velocity of vapor in heat pipe [m s^{-1}]
v	velocity of heat pipe [m s^{-1}]
v_{min}	critical working velocity of heat pipe [m s^{-1}]
V_l	liquid volume in heat pipe [m^3]
V_{hp}	heat pipe volume [m^3].

Greek symbols

ρ_l	liquid density [kg m^{-3}]
ρ_v	vapor density [kg m^{-3}]
θ	declination angle of reciprocating heat pipe [degree]
ω	angular velocity of engine crank [rad s^{-1}]
ω_{min}	critical working angular velocity of engine crank [rad s^{-1}].

section, and thus the heat pipe ceases to function. This minimum reciprocating frequency at which liquid can continuously reach the evaporator section and, therefore, the heat pipe can work steadily is also defined as the critical working frequency of the heat pipe. The major objective of this paper is to study this critical working frequency both analytically and experimentally for various axially reciprocating mechanisms.

ANALYTICAL SOLUTIONS FOR THE CRITICAL WORKING FREQUENCY

Since the reciprocating heat pipe is installed in the reciprocating element, the motion of the heat pipe is the same as the reciprocal motion of the element. For generality, an offset slider–crank mechanism with an upright slider and a wickless reciprocating heat pipe is studied (as shown in Fig. 2). Consider a typical liquid particle which is initially at the surface of the liquid on the bottom of the heat pipe when the heat pipe begins to move upwards from the lowest point. The motion of the slider/heat-pipe combination is confined within the dead ends of the slider. When the heat pipe moves upwards, it carries the liquid particle with it at the same time. Therefore, the liquid particle has the same velocity as that of the heat pipe during the initial period of the upward stroke. Due to the reciprocating characteristics of the slider–crank mechanism, the velocity of the heat pipe will reach the maximum value and the corresponding acceleration of the heat pipe will become zero when the heat pipe reaches a certain location corresponding to time, $t = t_0$. At this time, t_0, the liquid particle begins to separate from the bottom of the heat pipe. For $t > t_0$, the acceleration of the heat pipe becomes negative, and the heat pipe velocity is gradually reduced. The velocity of the heat pipe will be zero when the heat pipe reaches the upper dead end. Since the motion of the liquid particle is not controlled by the crank–slider mechanism after the separation, the liquid particle is subject only to the gravitational force and resistant forces acting on the liquid particle. At the separating time, t_0, the initial velocity of the liquid particle is equal to the velocity of the heat pipe. After the separation, the velocity of the liquid particle will be initially higher than that of the heat pipe, since the heat pipe velocity is reduced much faster than that of the liquid

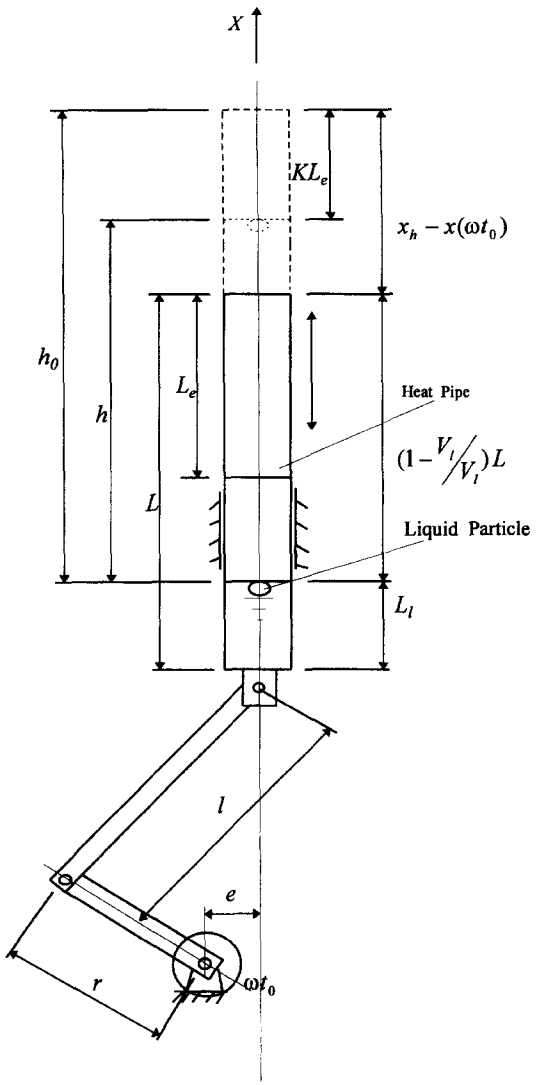

Fig. 2. Schematic of reciprocating mechanism with a heat pipe.

particle due to the reciprocating motion of the mechanism. However, the particle velocity will also be gradually reduced due to the effect of gravity and resistant forces. Consider a particular moment in the fixed Newtonian coordinate system when the heat pipe moves up to the upper dead end, x_h, from the separation point $x(\omega t_0)$. If at the same time the liquid particle just reached the top end of the heat pipe when its velocity is reduced to zero, the absolute displacement, h_0, of the liquid particle from the separation point is the superposition of the displacement of the particle relative to the heat pipe and the displacement of the heat pipe itself, as shown in Fig. 2. Therefore, h_0 can be expressed by the following equation:

$$h_0 = \left(1 - \frac{V_l}{V_{hp}}\right) L + [x_h - x(\omega t_0)] \tag{1}$$

where x_h and $x(\omega t_0)$ are, respectively, the upper dead end and separation position of the heat pipe. V_l and V_{hp} are the liquid charge volume and the total heat pipe interior volume, respectively, and L is the length of heat pipe. However, even if the liquid particle could return only to a certain location in the evaporator section instead of the top end, the heat pipe may still work steadily due to the axial heat conduction along the container wall. Therefore, the actual displacement required for the liquid particle may be smaller than that given by equation (1), and may be expressed as:

$$h = h_0 - kL_e \tag{2}$$

where L_e is the length of the evaporator section and k is the location coefficient, $0 \leqslant k \leqslant 1$. k is zero when the liquid particle reaches the top end of the evaporator section, and is unity when the liquid particle could just reach the bottom end of the evaporator section. If the reciprocating heat pipe is installed with an inclination angle θ, the following equation can be obtained through the conservation of energy in the Newtonian coordinate system, when the resistant forces are neglected as a first approximation:

$$\tfrac{1}{2} m_p v_{min}^2 = m_p g h \cos\theta \tag{3}$$

where m_p is the mass of the liquid particle and v_{min} is the velocity of the liquid particle at the separation time, t_0, which is the same as the heat pipe velocity at the separation.

For different reciprocating mechanisms, the values of v_{min} and h in equation (3) are different. For the offset slider–crank mechanism, as shown in Fig. 1(a), the dimensionless displacement of the heat pipe is of the form:

$$\frac{x}{r} = \cos\omega t + \frac{1}{r}\sqrt{l^2 - e^2 - r^2\sin^2\omega t - 2er\sin\omega t}. \tag{4}$$

The dimensionless velocity and acceleration of the heat pipe are then, respectively:

$$\frac{v}{r\omega} = \frac{1}{r\omega}\frac{dx}{dt} = -\sin\omega t - \frac{r\sin 2\omega t + 2e\cos\omega t}{2\sqrt{l^2 - e^2 - r^2\sin^2\omega t - 2er\sin\omega t}} \tag{5}$$

$$\frac{a}{r\omega^2} = \frac{1}{r\omega^2}\frac{dv}{dt} = -\cos\omega t - \frac{r\cos 2\omega t - e\sin\omega t}{\sqrt{l^2 - e^2 - r^2\sin^2\omega t - 2er\sin\omega t}} - \frac{1}{4}\frac{r^3\sin^2 2\omega t + 4er^2\sin 2\omega t\cos\omega t + 4e^2 r\cos^2\omega t}{(l^2 - e^2 - r^2\sin^2\omega t - 2er\sin\omega t)^{1.5}}. \tag{6}$$

Therefore, the following equations for the displacement difference in equation (1) can be obtained:

$$x_h - x(\omega t_0) = \sqrt{(l+r)^2 - e^2} - r\left(\cos\omega t_0 + \frac{1}{r}\sqrt{l^2 - e^2 - r^2\sin^2\omega t_0 - 2er\sin\omega t_0}\right). \quad (7a)$$

Substituting equation (7a) into equation (2) yields:

$$h = \left(1 - \frac{V_l}{V_{hp}}\right)L + \sqrt{(l+r)^2 - e^2} - r\left(\cos\omega t_0 + \frac{1}{r}\sqrt{l^2 - e^2 - r^2\sin\omega t_0 - 2er\sin\omega t_0}\right) - kL_e. \quad (7b)$$

The critical working velocity, v_{min}, in equation (3) can be found from equation (5) at the separation point ωt_0:

$$v_{min} = -r\omega_{min}\left(\sin\omega t_0 + \frac{\frac{1}{2}r\sin 2\omega t_0 + e\cos\omega t_0}{\sqrt{l^2 - e^2 - r^2\sin^2\omega t_0 - 2er\sin\omega t_0}}\right). \quad (8)$$

The critical angular velocity and the critical working frequency in equation (8) are related through the following equation:

$$\omega_{min} = 2\pi f_{min} \quad (9)$$

Substituting equations (7b), (8) and (9) into equation (3), and rearranging it, the critical frequency can be expressed by the following equation:

$$f_{min} = \frac{A}{\pi r}\sqrt{\frac{1}{2}gh\cos\theta} \quad (10)$$

where

$$A = -\left(\sin\omega t_0 + \frac{\frac{1}{2}r\sin 2\omega t_0 + e\cos\omega t_0}{\sqrt{l^2 - e^2 - r^2\sin^2\omega t_0 - 2er\sin\omega t_0}}\right)^{-1}.$$

Equation (10) is the analytical solution for the critical working frequency when the flow resistance and surface tension acting on the liquid particle is negligible. The crank angular position, ωt_0, at separation in equation (10) is a constant, and it can be found from equation (6) by setting the acceleration to be zero:

$$-\cos\omega t_0 - \frac{r\cos 2\omega t_0 - e\sin\omega t_0}{\sqrt{l^2 - e^2 - r^2\sin^2\omega t_0 - 2er\sin\omega t_0}} - \frac{1}{4}\frac{r^3\sin^2 2\omega t_0 + 4er^2\sin 2\omega t_0\cos\omega t_0 + 4e^2 r\cos^2\omega t_0}{(l^2 - e^2 - r^2\sin^2\omega t_0 - 2er\sin\omega t_0)^{1.5}} = 0. \quad (11)$$

If offset $e = 0$, the offset slider–crank mechanism is reduced to the on-center slider–crank mechanism as shown in Fig. 2(b) and the relation for the critical working frequency is readily obtained:

$$f_{min} = \frac{1}{\pi r}\frac{1}{-\sin\omega t_0 - \frac{1}{2}\frac{r\sin 2\omega t_0}{\sqrt{l^2 - r^2\sin^2\omega t_0}}}\sqrt{\frac{g}{2}h\cos\theta}. \quad (12)$$

Equation (12) is the analytical solution for the on-center slider–crank mechanism when the flow resistance and surface tension acting on the liquid particle is negligible. The crank angular position ωt_0 in equation (12) is a constant, and it can be found from equation (6) by setting the acceleration to be zero at $e = 0$:

$$-\cos\omega t_0 - \frac{r\cos 2\omega t_0}{\sqrt{l^2 - r^2\sin^2\omega t_0}} - \frac{1}{4}\frac{r^3\sin^2 2\omega t_0}{(l^2 - r^2\sin^2\omega t_0)^{3/2}} = 0. \quad (13)$$

If the connecting rod length $l \gg r$ and e, equations (4)–(6) can be simplified to the following forms:

$$x = r\cos\omega t + l \quad (14)$$

$$v = -r\omega\sin\omega t \quad (15)$$

$$a = -r\omega^2\cos\omega t. \quad (16)$$

The motion of the heat pipe, therefore, becomes the harmonic motion. If the connecting rod length is zero, the mechanism is called the Scotch yoke mechanism, as shown in Fig. 1(c). The motion of the heat pipe in the Scotch yoke mechanism is a pure harmonic motion, and the corresponding dimensionless displacement becomes:

$$\frac{x}{r} = \cos\omega t. \quad (17)$$

The dimensionless velocity and acceleration of the heat pipe are similar to equations (15) and (16). Similarly, substituting the above displacements, velocities, and accelerations into equations (1)–(3), and rearranging them, we then obtain:

$$h = \left(1 - \frac{V_l}{V_{hp}}\right)L + r(1 - \cos\omega t_0) - kL_e \quad (18)$$

$$v_{min} = -r\omega_{min}\sin\omega t_0 \quad (19)$$

$$f_{min} = -\frac{1}{\pi r\sin\omega t_0}\sqrt{\frac{1}{2}gh\cos\theta} \quad (20)$$

$$\cos\omega t_0 = 0. \quad (21)$$

The values of ωt_0 for all three typical mechanisms should be taken within $180° \leqslant \omega t_0 \leqslant 360°$, corresponding to the upward motion of the heat pipe. The values of the heat-pipe inclination angle are $0° \leqslant \theta \leqslant 90°$. For a general heat-pipe design, the value of k in equation (2) can be taken as 0.5, which corresponds to the middle section of the evaporator.

It should be pointed out that the above analytical relations are derived based on the three typical axially reciprocating mechanisms shown in Fig. 1. However, for any other axially reciprocating mechanisms, if their displacement, velocity, and acceleration are known, the analytical solutions for the critical working frequency of the heat pipe can also be obtained based on equations (1)–(3). The reciprocating heat pipe can work steadily if the working frequency of heat pipe is higher than the critical working frequency.

SEMI-EMPIRICAL CORRELATION FOR THE CRITICAL WORKING FREQUENCY

The analytical solutions presented in the earlier section are based on the assumption that the flow resistance and surface tension are negligible. In practice, a liquid particle traveling in the heat pipe is subjected to various resistant forces, such as those due to vapor flow, other liquid particles, and the container wall, in addition to the gravitational force. In this section, these resistant forces are included in the analysis. Based on conservation of energy, the motion of a typical liquid particle in Fig. 2 can be described by the following equation:

$$\tfrac{1}{2}m_p v_{\min}^2 = m_p g h' \cos\theta + F_R h' \tag{22}$$

where F_R is the total resistance acting on the liquid particle, h' is the absolute displacement of the liquid particle from the separation point to a certain location of the evaporator section, when the effect of resistant force is taken into consideration.

For the on-center slider–crank mechanism, as described through equations (4) and (5), the velocity $v_{\min}$ of the heat pipe is proportional to $r\omega_{\min}$, i.e.:

$$v_{\min} = \sqrt{C} r\omega_{\min} \tag{23}$$

where C is a proportionality constant. h' is related to h through another constant, C_1:

$$h' = C_1 h. \tag{24}$$

Substituting equations (23) and (24) into (22) yields:

$$\frac{1}{2}Cr^2\omega_{\min}^2 = C_1\left(g\cos\theta + \frac{F_R}{m_p}\right)h. \tag{25}$$

In fact, the total flow resistant force acting on the liquid particle consists of the frictional force and vapor drag force, i.e.:

$$F_R = F_f + F_v. \tag{26}$$

The frictional force can be expressed by the equation of the form [9]:

$$F_f = C_0\tau_s A_{p,s} = \tfrac{1}{2}C_0\rho_l u_m^2 C_f A_{p,s} \tag{27}$$

where u_m is the mean velocity of the particle in the heat pipe, which can be expressed as:

$$u_m = B_1 r\omega_{\min}. \tag{28}$$

Substituting equation (28) into equation (27) yields:

$$F_f = \tfrac{1}{2}B_1 C_0\rho_l C_f A_{p,s} r^2\omega_{\min}^2 \tag{29}$$

where $A_{p,s}$ is the lateral area of the heat pipe, C_f is the frictional coefficient, C_0 and B_1 are constants, and ρ_l is the liquid density.

The vapor drag force can be expressed by the following relation [9]:

$$F_v = \tfrac{1}{2}C_D\rho_v u_{v,m}^2 A_{p,v} \tag{30}$$

where $A_{p,v}$ is the frontal area of the liquid particle, C_D is the drag coefficient, and $u_{v,m}$ is the mean velocity of the vapor in the heat pipe which can be expressed in terms of the total heat input in the evaporator section:

$$u_{v,m} = \frac{C_2 Q}{\rho_v A_{hp} h_{fg}} \tag{31}$$

where C_2 is a proportionality coefficient, A_{hp} is the cross-sectional area of heat pipe, ρ_v is the vapor density, h_{fg} is the latent heat of vaporization, and Q is the total heat input of the heat pipe. Substitution of equation (31) into equation (30) results in:

$$F_v = \frac{1}{2}C_D C_2 \frac{A_{p,v}}{\rho_v A_{hp}^2}\frac{Q^2}{h_{fg}^2}. \tag{32}$$

Finally, combining equations (29)–(32) with equation (25), we obtain:

$$\frac{1}{2}Cr^2\omega_{\min}^2 = C_1 gh\cos\theta + \frac{C_1 h}{m_p}\left(\frac{1}{2}B_1 C_0 C_f A_{p,s} r^2\omega_{\min}^2 + \frac{1}{2}C_D C_2 \frac{A_{p,v}}{\rho_v A_{hp}^2}\frac{Q^2}{h_{fg}^2}\right) \tag{33}$$

where $m_p = B_2 m_l = B_2 V_l\rho_l = (B_2\pi/4)d^2 L_l\rho_l$, $A_{p,s} = B_3 A_S = B_3\pi d L_l$, $A_{p,v} = B_4 A_{hp}$, m_l is the total liquid mass in the heat pipe, A_s is the lateral area of liquid volume in the heat pipe, and L_l is the height of liquid volume in the heat pipe. Equation (33) can be rearranged into the following form:

$$\frac{1}{2}Cr^2\omega_{\min}^2 = C_1 gh\cos\theta + \frac{2B_1 B_3 C_0 C_1 C_f}{B_2}\frac{h}{d}r^2\omega_{\min}^2 + \frac{B_4 C_1 C_2 C_D}{2B_2}\frac{h}{L}\frac{1}{V_l/V_{hp}}\frac{1}{\rho_l/\rho_v}\frac{Q^2}{A_{hp}^2 h_{fg}^2}. \tag{34}$$

Since $\omega_{\min} = 2\pi f_{\min}$, equation (34) can be re-written in a more explicit equation of the form:

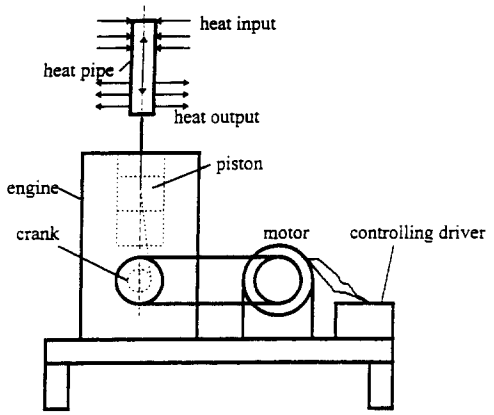

Fig. 3. Schematic of the heat pipe test apparatus.

$$f_{\min} = \frac{1}{r}\sqrt{\frac{gh\cos\theta + D_3\dfrac{h}{L}\dfrac{V_{hp}}{V_l}\dfrac{1}{\rho_l\rho_v}\dfrac{Q^2}{A_{hp}^2 h_{fg}^2}}{D_1 - D_2\dfrac{h}{d}}} \quad (35)$$

where

$$D_1 = \frac{2\pi^2 C}{C_1}, \quad D_2 = \frac{8\pi^2 B_1 B_3 C_0 C_f}{B_2},$$

$$\text{and} \quad D_3 = \frac{B_4 C_2 C_D}{2B_2}$$

are constants that should be determined by experimental data.

EXPERIMENTAL APPARATUS AND RESULTS

The test apparatus for reciprocating heat pipes is shown in Fig. 3, whose structure and working mechanism have been presented elsewhere [10]. Four copper–water heat pipes with different diameters, lengths, and ratios of the charged water volume to the heat pipe volume were fabricated and tested. The diameters of the heat pipes varied from 7.75 to 10.92 mm, the lengths of the heat pipes varied from 100 to 200 mm, and the ratios of the water charge to the heat pipe volume varied from 9.54 to 41.6%. The upper halves of the heat pipes were wrapped with a flexible electric heater, which worked as evaporators, and were insulated by the insulation material on the outer surface. The lower halves of the heat pipes, which worked as condensers, were cooled by air during the reciprocating motion of the heat pipes. The temperature distribution along the heat pipe was measured using four thermocouples. The uncertainty associated with the measured temperature was estimated to be $\pm 0.5\%$, and the heat input uncertainty was estimated to be ± 3 W. The heat pipes worked initially at higher working frequency, which was then gradually reduced through the motor controlling driver. As the reciprocating motion was decreased, the heat pipe performance continued to deteriorate until the temperature drops of heat pipes rose sharply (more than

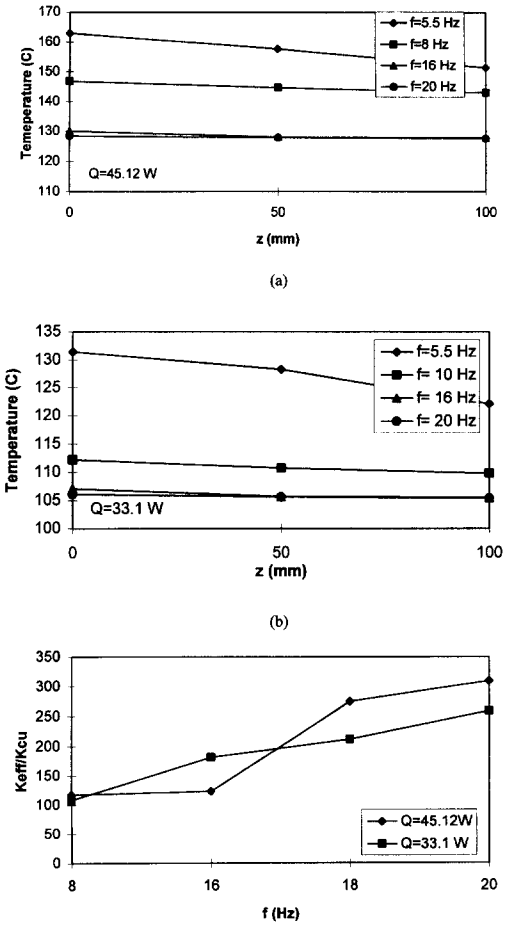

Fig. 4. Temperature distributions and effective thermal conductances of the heat pipe with $L = 100$ mm, $d = 7.75$ mm, and ratio = 23.74%.

30°C), and the heat pipe could no longer retain a stable working condition. It was believed that the heat pipes reached their working limit at this condition, and the power input to the heat pipes were shut down immediately in order to avoid burn-out of the heat pipes. The lowest reciprocating frequency which could sustain a stable heat pipe operation above this burn-out point was considered to be the critical working frequency of the heat pipe.

Figure 3(a–c) presents some representative testing results in terms of temperature distributions along the heat pipe length and the effective thermal conductance. As shown in Fig. 3(a, b), the temperature distribution was rather uniform when the working frequency is relatively high, indicating that the heat pipe worked very well. When the working frequency was gradually decreased, the temperature drop along the heat pipe increased accordingly. When the working frequency was reduced to about 5.5 Hz, the temperature drop increased to more than 15°C. Temperature fluctuation also occurred in this condition, and the working limitation was being reached. Figure 3(c) shows the ratio of the heat-pipe effective thermal

conductance to the copper thermal conductivity, taken to be 380 W m^{-1} $°C^{-1}$, at different working frequencies. As can be seen, the effective thermal conductance reaches more than 300 times that of copper with a moderate working frequency, indicating that the heat pipe is a very effective heat-transfer device.

COMPARISON OF ANALYTICAL AND EXPERIMENTAL RESULTS

In order to establish the applicability of the analytical solution, the analytical results are compared with the corresponding experimental data. For the test apparatus shown in Fig. 3, the offset e is zero, the crank-radius length r is 35 mm, and the connecting rod length l is 104.8 mm. Substituting these values into equation (13) results in $\omega t_0 \approx 287°$. If the absolute displacement h is known, the analytical solution of the critical working frequency as a function of the heat pipe length and ratio of the fluid charge can be determined through equation (12). In practice, heat pipes could still work to a certain extent if the liquid particle could return only to some location of evaporator section lower than the evaporator end cap, due to the axial heat conduction in the heat pipe wall. However, since this axial heat conduction effect is very difficult to quantify, several typical locations in the evaporator section were chosen for the evaluation of the absolute displacement, which is reflected through the value of location coefficient k. For the same heat pipe length and ratio of water charge at $\theta = 0°$, the analytical and experimental results are presented and compared in Table 1. From Table 1, it can be seen that the analytical frequencies are higher than the experimental results if $k = 0$ and 0.5 are assumed. If the liquid particle only reaches the bottom of evaporator section (i.e. $k = 1$), the analytical frequency is much lower than the experimental result. Therefore, it is clear that the actual location corresponding to the heat transfer limit should be in between the middle and bottom sections of the evaporator (i.e. $0.5 < k < 1$). If k is assumed to be 0.75, the analytical solution is reasonably smaller than experimental results, and the maximum error is only about -9.56%. This comparison indicates that the critical working frequency is reached when the liquid particle can only return to the lower middle section of the evaporator. It should be pointed out that although $k = 0.75$ gives a more accurate analytical solution, $k = 0.5$ gives a more convenient and conservative calculation for the heat pipe design. The agreement between the analytical and experimental results are also excellent (Table 1). Even for $k = 1$ or 0, the discrepancy between the analytical solutions and experimental data are still relatively small. Considering the extremely complicated problem in this study, the analytical solutions predict the critical working frequency accurately for any values of k between 0 and 1.

The experimental data were also used to determine the constants in the semi-empirical correlation for the critical working frequency with the assistance of a linear regression analyses. The ranges of data are as follows:

$$100 \text{ mm} \leqslant L \leqslant 200 \text{ mm}, \quad 7.75 \text{ mm} \leqslant d \leqslant 10.9 \text{ mm},$$

$$23.7\% \leqslant \frac{V_l}{V_{hp}} \leqslant 40\%,$$

Table 1. Comparison of analytical results and experimental data, $\theta = 0°$

L [mm]	L_e [mm]	d [mm]	Ratio [%]	Q [W]	Analytical $k = 0$ [Hz]	Analytical $k = 0.5$ [Hz]	Analytical $k = 0.75$ [Hz]	Analytical $k = 1.0$ [Hz]	Exp data [Hz]	Errors $k = 0.5$ [%]
100	50	7.75	23.7	20.1	6.23	5.54	5.02	4.54	5.6	−1.1
100	50	7.75	23.7	27.1	6.23	5.54	5.02	4.54	5.6	−1.1
100	50	7.75	23.7	35.3	6.23	5.54	5.02	4.54	5.5	0.7
100	50	7.75	23.7	39.8	6.23	5.54	5.02	4.54	5.5	0.7
100	50	7.75	23.7	43.9	6.23	5.54	5.02	4.54	5.5	0.7
100	50	7.75	23.7	47.0	6.23	5.54	5.02	4.54	5.5	0.7
100	50	7.75	23.7	53.8	6.23	5.54	5.02	4.54	5.5	0.7
100	50	10.92	40.0	21.1	5.74	4.88	4.39	3.83	4.6	5.7
100	50	10.92	40.0	30.8	5.74	4.88	4.39	3.83	4.6	5.7
100	50	10.92	40.0	39.1	5.74	4.88	4.39	3.83	4.6	5.7
100	50	10.92	40.0	42.0	5.74	4.88	4.39	3.83	4.6	5.7
100	50	10.92	40.0	47.5	5.74	4.88	4.39	3.83	4.5	7.8
150	75	7.75	30.0	18.5	7.04	6.06	5.49	4.9	6.1	−0.7
150	75	7.75	30.0	24.8	7.04	6.06	5.49	4.9	6.1	−0.7
150	75	7.75	30.0	30.7	7.04	6.06	5.49	4.9	6.0	1.0
150	75	7.75	30.0	38.7	7.04	6.06	5.49	4.9	6.0	1.0
150	75	7.75	30.0	47.7	7.04	6.06	5.49	4.9	6.0	1.0
200	100	7.75	30.0	23.0	7.9	6.8	6.12	5.53	6.4	5.9
200	100	7.75	30.0	32.5	7.9	6.8	6.12	5.53	6.4	5.9
200	100	7.75	30.0	40.1	7.9	6.8	6.12	5.53	6.3	7.4
200	100	7.75	30.0	50.5	7.9	6.8	6.12	5.53	6.3	7.4
200	100	7.75	30.0	61.3	7.9	6.8	6.12	5.53	6.3	7.4

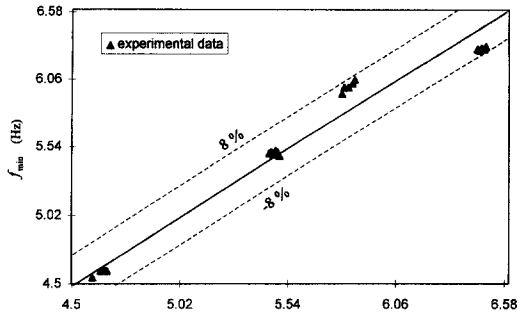

$$\frac{1}{r}\sqrt{\frac{gh+96.1\dfrac{h}{L}\dfrac{1}{V_l/V_{hp}}\dfrac{1}{\rho_l\rho_v}\dfrac{Q^2}{A_{hp}^2h_{fg}^2}}{19.9-0.086\dfrac{h}{d}}} \quad \text{(Hz)}$$

Fig. 5. Comparison between the correlation and experimental data for the critical working frequency ($k = 0.5$, $Q = 20.1$–61.3 W).

$$18.7\ \text{W} \leqslant Q \leqslant 61.3\ \text{W}, \quad k = 0.75, \quad \text{and} \quad \theta = 0^\circ.$$

The empirical constants thus determined in equation (35) are: $D_1 = 19.9$, $D_2 = 0.086$, and $D_3 = 96.1$. Substituting them into equation (35), the final form of the critical working frequency is obtained:

$$f_{\min} = \frac{1}{r}\sqrt{\frac{gh+96.1\dfrac{h}{L}\dfrac{1}{V_l/V_{hp}}\dfrac{1}{\rho_l\rho_v}\dfrac{Q^2}{A_{hp}^2h_{fg}^2}}{19.9-0.086\dfrac{h}{d}}} \tag{36}$$

where

$$h = \left(1-\frac{V_l}{V_{hp}}\right)L + r\left[1-\left(\cos\omega t_0 + \frac{1}{r}\sqrt{l^2-r^2\sin^2\omega t_0}-\frac{l}{r}\right)\right]-kL_e, \quad \theta = 0^\circ$$

and $0 \leqslant k \leqslant 1$.

The semi-empirical correlation are compared with the corresponding experimental data in Fig. 5 with a maximum error of only about 7.8%.

CONCLUSIONS

An analytical and experimental investigation on the critical working frequency of reciprocating heat pipes has been conducted. Analytical solutions for various reciprocating mechanisms and a semi-empirical correlation at offset $e = 0$ have been obtained through mathematical modeling and experimental measurement. The theoretical solution and experimental results show that the critical working frequencies for various heat pipes ($L = 100$–200 mm) are very low. Even for an engine–crank radius of $r = 35$ mm, the critical working frequencies are only on the order of 5–7 Hz. Therefore, the reciprocating heat pipe is well suited for the engine piston application. The analytical solutions and semi-empirical correlation predict the critical working frequency remarkably well and provide useful tools for the design of reciprocating heat pipes in various axially reciprocating mechanisms.

Acknowledgements—The authors would like to acknowledge the Office of Naval Research and the National Science Foundation for the financial support.

REFERENCES

1. Cao, Y. and Wang, W., Reciprocating heat pipes and their applications. *ASME Journal of Heat Transfer*, 1995, **117**, 1094–1096.
2. Wang, Q., Cao, Y. and Souto, A., Development of a new engine piston incorporating heat pipe cooling technology. SAE paper no. 950521, 1995.
3. Cotter, T. P., Theory of heat pipes, Los Alamos Science Laboratory Report no. LA-3246-MS, 1965.
4. Tien, C. L., Fluid mechanics of heat pipes. *Annual Review Fluid Mechanics*, 1975, **7**, 167–185.
5. Marto, P., Performance characteristics of rotating wickless heat pipes. *Proceedings of the 2nd IHPC*, Bologna, Italy, 1976, pp. 281–291.
6. Faghri, A., *Heat Pipe Science and Technology*. Taylor and Francis, Washington, D.C., 1995, pp. 115–215.
7. Cao, Y., Wang, Q. and Ling, J., Operating limitation of reciprocating heat pipes for piston cooling applications. *ASME Winter Conference*, **1**. San Francisco, 1995, pp. 235–241.
8. Ling, J., Analytical and experimental investigations of reciprocating heat pipes. Master's Thesis, Florida International University, Miami, FL, 1995.
9. Incropera, F. P. and Dewitt, D. P., *Introduction to Heat Transfer*. Wiley, New York, 1990.
10. Ling, J., Cao, Y. and Wang, Q., Experimental investigations and correlations for the performance of reciprocating heat pipes. *Journal of Heat Transfer Engineering*, 1996, **17**(4), 34–35.